5 GHz Channel Spacing InP-Based 32-Channel Arrayed-Waveguide Grating

W. Jiang[1], K. Okamoto[1], F. M. Soares[1], F. Olsson[2], S. Lourdudoss[2], and S. J. B. Yoo[1]
Department of Electrical and Computer Engineering[1], University of California, Davis, 95616
Department of Microelectronics and Information Technology[2], Royal Institute of Technology, Sweden
email: yoo@ece.ucdavis.edu

Abstract: We realize a 32-channel InP-based Arrayed-Waveguide Grating (AWG) with a 5-GHz channel spacing. The AWG shows approximately 14 dB excess-loss, 9 dB crosstalk, and 21 × 22 mm^2 dimensions.

OCIS codes: (130.3120) Integrated optics devices; (130.5990) Semiconductors.

1. Introduction

Wavelength multiplexing and demultiplexing components with high-resolution channel spacing are indispensible for ultrahigh-density WDM systems. So far, silica-based AWGs have already achieved channel spacing down to 1 GHz [1]. On the other hand, InP-based high-resolution AWGs are particularly attractive for integration with other active photonic devices such as mode-locked lasers [2] and photodetectors. Monolithically integrated high-resolution InP-based AWGs will have various applications, such as multi-wavelength laser arrays [3], optical spectrum analyzers, and optical arbitrary waveform generators (OAWG) [4]. Recently, we have successfully realized InP-based AWGs with channel spacing of 20 GHz and 10 GHz [5]. In this paper, we report an InP-based AWG with a channel spacing of 5 GHz.

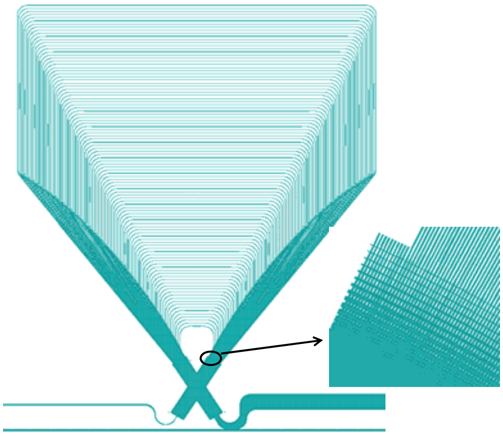

a)

Number of Channels	32
Number of Arrayed Arms	104
Channel spacing (GHz)	5
Free spectral range (GHz)	160
Grating order	1095
Path length difference Δ L (μm)	527.142
Radius of slab region (μm)	3198.384
Bend radius of arrayed arms (μm)	500
Chip size (mm×mm)	21 × 22

b)

Fig. 1 (a) Layout of the 5GHz channel-spacing AWG, and (b) a table of the main design parameters.

2. Design

The major challenge of realizing high-resolution AWGs lies in the ability to maintain the constant phase difference between the optical signals propagating through the adjacent array arms. While the path length difference ΔL becomes increasingly longer as channel spacing becomes narrower, the constant phase relation will suffer from fabrication limitations, such as variations in the waveguide width as well as variations in the core-layer-composition and thickness. The induced phase errors over the array arms can severely degrade the transmission of high-resolution AWGs and increases the crosstalk. Also, due to the large dimension of the device, loss becomes another issue of realizing high-resolution AWGs. This paper discusses the design and fabrication of a relatively low-loss fabrication-error-tolerant 5-GHz AWG.

Fig. 1 (a) shows the mask layout of the 5-GHz AWG, and (b) a table of the key design parameters. The AWG includes 3 input waveguides, 32 output waveguides, and 104 array arms with a path length difference ΔL of 527.142 μm between the adjacent arms. The diffraction order at λ = 1.552 μm is 1095, which results in a free spectral range (FSR) of 160 GHz. The gap between the adjacent arrayed waveguides at the edge of the slab region is 0.8 μm, which is the smallest lithographic resolution of our fabrication process.

The waveguides consist of buried hetero-structure (BH) waveguides, which show a higher tolerance to core-width and thickness variations, due to the lower index contrast as compared to other types of high-contrast waveguides, such as high-mesa waveguides. The box geometry is used with two slab regions crossing each other to reduce the total size of the AWG. Importantly, we carefully design the arrayed waveguides (AWs) in order to increase the phase-error tolerance. The 3-μm-wide bends have a large radius-of-curvature (R=500 μm), to prevent first-order mode excitation from straight to curved waveguide transitions. An equal bending radius of R=500 μm was imposed for all AWs, such that any systematic phase errors in the bending waveguides will be constant for all AWs. For the straight section of AWs, a waveguide width of 5 μm is chosen instead of the conventional width of 3 μm, because of two advantages. First, the dependence of the propagation constant on waveguide width for 5-μm width is 3.7 times smaller than that for 3-μm width (shown in Fig. 2a), therefore the phase errors due to variations in the waveguide width can be reduced. In addition, the broader waveguide width can result in the lower propagation loss. In order to prevent the multi-mode effect in the 5-μm-wide waveguide (up to 4 guided modes for TE), an adiabatic taper from 5 μm to 3 μm is inserted between the broad straight section and the bending curve.

In order to reduce the insertion loss of the AWG, a segmented transition region [6] is inserted between the slab region and the arrayed waveguides (shown in the inset of Fig. 1a), which comprises 15 paths intersecting the waveguide array and exhibiting progressively decreasing width as they depart further away from the slab.

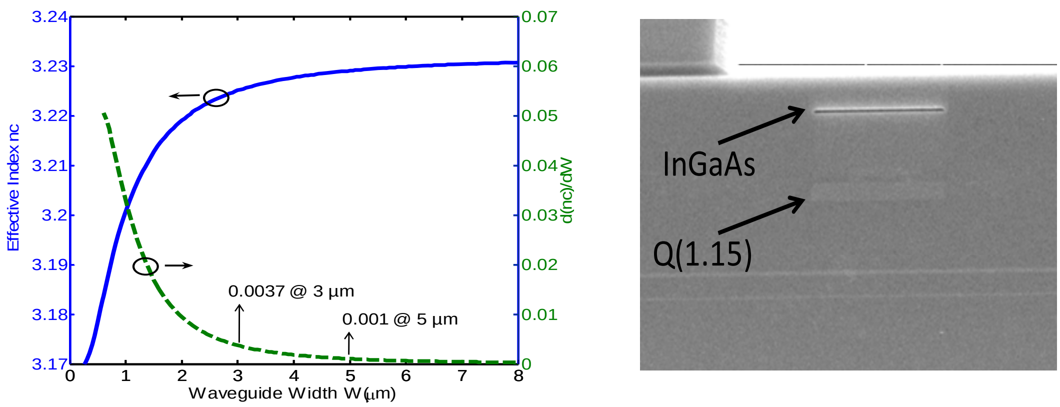

a) b)

Fig. 2 (a) the dependence of the effective refractive index on waveguide width for the BH waveguide, and (b) an SEM photo of the BH waveguide.

3. Fabrication

Figure 2(b) shows an SEM photo of the BH waveguide. The epitaxial wafer was grown on an InP substrate by metal-organic-vapor-phase-epitaxy (MOVPE). The waveguide structure consists of a 2-μm n-doped InP lower-cladding layer, a 0.5-μm Q(1.15) waveguide core layer, a 2-μm p-doped InP top cladding layer, and a 0.2-μm p-doped InGaAs layer. The thin InGaAs layer was added for testing purposes and does not influence the waveguiding properties. After photo-lithographic patterning, waveguides were etched in a Br_2/N_2 reactive-ion-etcher using a 550-nm SiO_2 layer as mask. Subsequently, the SiO_2 mask was selectively removed in a buffered hydrofluoric-acid solution. Then, Fe-doped semi-insulating InP was regrown by low pressure hydride vapor phase epitaxy (HVPE), resulting in the BH waveguide.

4. Results and Discussion

The measurement setup is as follows. Light from a tunable laser source (TLS) is passed through a polarization controller, and launched into one of the inputs of the AWG by coupling in with a lensed fiber. At the output of the AWG, the light is collimated by a microscope objective and passed through a pinhole, and a TE polarizer. After the polarizer, the light is focussed onto a photo detector (PD). The spectral response of the AWG is obtained by measuring the optical power in the PD, while sweeping the wavelength of the TLS. The transmission is calibrated against straight reference 3-μm waveguides. Fig. 2a shows the spectral response of the 5-GHz AWG over 32 channels for TE polarization, with an excess loss of approximately 14 dB and a crosstalk level of approximately 9 dB. The optical power from channel 25 is much weaker than others due to the bad output waveguide. We have also measured the phase errors over all 104 array arms (shown in Fig. 3b) with an optical vector network analyzer (OVNA) which uses swept frequency-domain interferometry to characterize the complex transfer function and timedomain impulse response of the AWG in both amplitude and phase [7]. Later, phase-error compensation using electro-optic effect will be conducted to further reduce the crosstalk.

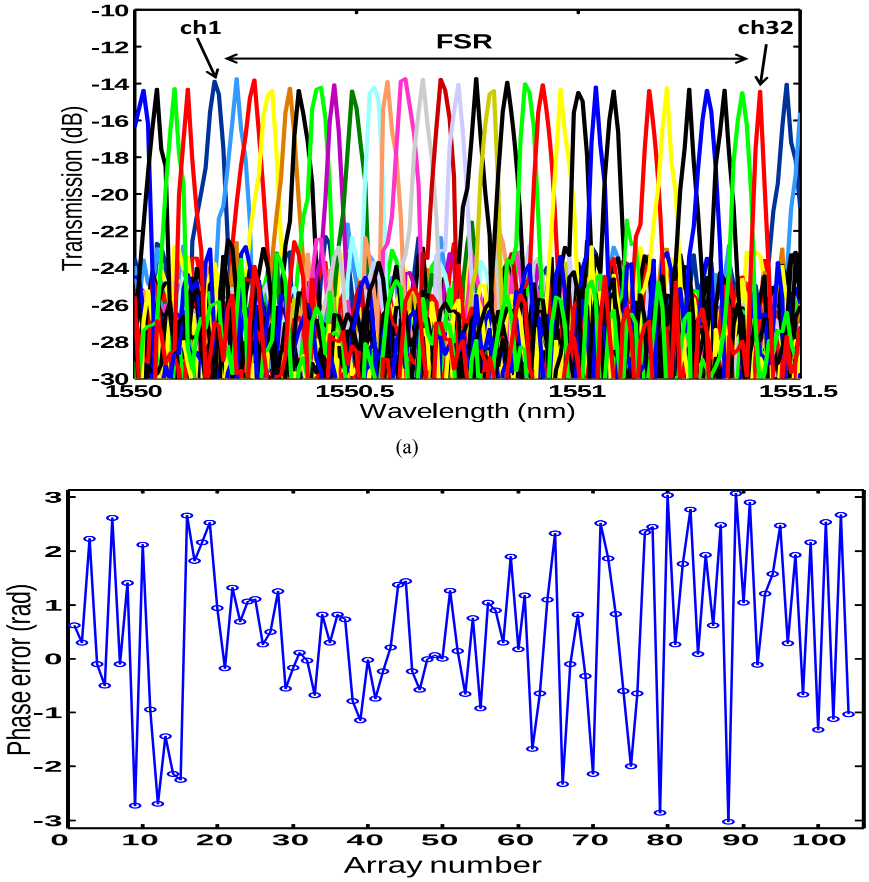

(a)

b)

Fig. 2 (a) Spectral response of the 5-GHz AWG over all 32 channels measured by sweeping light from a tunable laser, and (b) the phase errors over all 104 AWs measured with an OVNA.

4. Conclusions

We realized an InP-based 32-channel AWG with 5 GHz channel spacing using BH waveguides. The AWG design employed a 5µm-waveguide-width in straight sections of 104 AWs all with an equal bending radius of the same length to minimize phase errors. The size of the AWG was 21 mm × 22 mm, the crosstalk level was approximately 9 dB and the excess loss was 14 dB. With the measured phase errors, we are able to apply phase-error compensation on each array arm in the future.

5. References

[1] K. Takada, et al., "1-GHz-spaced 16-channel arrayed-waveguide grating for a wavelength reference standard in DWDM network systems," *J. Lightwave Technol.*, vol.20, no.5, pp. 850-853, May 2002.

[2] C. Ji, et al., "Synchronized Transform-limited Operation of 10 GHz Colliding Pulse Mode Locked Laser," *Photon. Technol. Lett.*, vol. 18, no. 4, pp. 625-627, Feb. 2006.

[3] R. Nagarajan, et al., "400 Gbit/s (10 channel × 40 Gbit/s) DWDM Photonic Integrated Circuits," *Electron. Lett.*, vol.41, no.6, pp.347-349, 17 March 2005.

[4] N. K. Fontaine, et al., "32 phase × 32 amplitude optical arbitrary waveform generation," *Opt. Lett.*, Vol. 32, No. 7, pp. 865-867, Apr. 2007.

[5] J. H. Baek, et al., "10 GHz and 20 GHz Channel Spacing High-resolution AWGs on InP," submitted to *Photon. Technol. Lett.*, Sep. 2008.

[6] W. Bogaerts, et al., "Compact Wavelength-Selective Functions in Silicon-on-Insulator Photonic Wires," *IEEE J. Select. Topics Quantum Electron.*, vol. 12, no. 6, 2006.

[7] Y. P. Li, US Patent No. 5,745,618 (1998).

[8] W. Jiang, et al., "Dynamic Phase-Error Compensation for High-Resolution InP Arrayed-Waveguide Grating Using Electro-optic Effect," *LEOS 2008*, no. MF2, Nov. 2008.

This work was supported in part by DARPA/SPAWAR under agreement number N66001-02-1-8937, and by DARPA/DSO OAWG under agreement number HR0011-05-C-0155.